Synthesis and Characterization of Poly(ethylene terephthalate)/Attapulgite Nanocomposites

Xuepei Yuan,[1,2] Chuncheng Li,[1] Guohu Guan,[1,2] Xiaoqing Liu,[1,2] Yaonan Xiao,[1] Dong Zhang[1]

[1]*CAS Key Laboratory of Engineering Plastics, Joint Laboratory of Polymer Science and Materials, Center for Molecular Science, Institute of Chemistry, The Chinese Academy of Sciences, Beijing 100080, People's Republic of China*
[2]*Graduate School of the Chinese Academy of Sciences, Beijing 100039, People's Republic of China*

Received 4 March 2006; accepted 29 July 2006
DOI 10.1002/app.25207
Published online in Wiley InterScience (www.interscience.wiley.com).

ABSTRACT: A kind of clay with fibrous morphology, attapulgite (AT), was used to prepare poly (ethylene terephthalate) (PET)/AT nanocomposites via *in situ* polymerization. Attapulgite was modified with Hexadecyltriphenylphosphonium bromide and silane coupling agent (3-glycidoxypropltrimethoxysilane) to increase the dispersion of clay particles in polymer matrix and the interaction between clay particles and polymer matrix. FTIR and TGA test of the organic-AT particles investigated the thermal stability and the loading quantity of organic reagents. XRD patterns and SEM micrographs showed that the organic modification was processed on the surface of rod-like crystals and did not shift the crystal structure of silicate. For PET/AT nanocomposites, it was revealed in TEM that the fibrous clay can be well dispersed in polymer matrix with the rod-like crystals in the range of nanometer scale. The diameter of rod-like crystal is about 20 nm and the length is near to 500 nm. The addition of the clay particles can enhance the thermal stability and crystallization rate of PET. With the addition of AT in PET matrix, the flexural modulus of those composites was also increased markedly. © 2006 Wiley Periodicals, Inc. J Appl Polym Sci 103: 1279–1286, 2007

Key words: poly(ethylene terephthalate); polyesters; nanocomposites; clay; attapulgite

INTRODUCTION

Since so called polymer-layered silicate nanocomposites were first prepared by Toyota group through dispersing a kind of layered clay into continuous nylon-6 matrix,[1–3] the steadily increasing attention has been paid to polymer nanocomposites, and various kinds of nanofillers have been chosen out for research. Different from the fillers in macro and microcomposites, at least one dimension of the dispersed fillers in nanocomposites is in the range of nanometer scale, typically 1–100 nm.[4–7] On the basis of the morphology or shape, the fillers can be classified into three categories in nanocomposites: (a) layered fillers, such as montmorillonite,[7–9] mica,[10] kaolinite,[11] and graphite,[12] which can be dispersed as layered, lamellar or lath-liked layers in polymer matrix with the thicknesses in several nanometers; (b) spheriform fillers such as nano-silica,[13] $BaSO_4$,[14] and TiO_2[15], whose three dimensions are in nanometer scale; (c) fibrous fillers such as carbon nanotubes[16] and carbon nanofibers.[17]

In these three categories of nanocomposites, the native layered clays or phyllosilicates as montmorillonites (MMT) have extensively been studied by lots of research groups.[4–9] Because of the crystal structure of layered clays, plenty of metal cations exist in their galleries between two layers. These metal cations can be exchanged by various long-chain organic cations, which helps to enlarge the interlayer spacing. However, the electrovalent bond still exists in the gallery and the silicate layers cannot be easily exfoliated thoroughly. On the other hand, compared with nylon, PET with less polar cannot strongly adhere to the silicates through ionic or hydrogen bonds.[18] Therefore, only intercalated PET/MMT nanocomposites could be obtained, and the enhancement of mechanical properties of those nanocomposites is limited. In the fibrous or rod-like nanofillers, carbon nanotubes and carbon nanofibers are widely studied because their high aspect ratio and outstanding Young's modulus are favorable to make excellent polymer–inorganic composites. Nevertheless, significant agglomeration, difficult surface-modification, and high cost obstruct their wide-ranging applications.[19,20]

Different from PET/MMT nanocomposites, another clay (attapulgite) with fibrous morphology in nanometer scale was used to synthesize PET nanocomposites in our studies. As a native mineral, attapulgite has the immense reserve in the world, and its processing is neither difficult nor expensive, which are useful for it to apply in industry. Then, this fibrous clay can be used as an attractive candidate for the expensive carbon nanotube and carbon nanofiber as fillers in nanocomposites.

Correspondence to: C.-C. Li (lizy@iccas.ac.cn).

Attapulgite, also called palygorskite usually, is a kind of phyllosilicate charactered by a microfibrous morphology, high surface charge, and large specific surface area. The structural formula of this clay minerals was first proposed by Bradley as $Mg_5Si_8O_{20}(OH)_4 \cdot 4H_2O$,[21] and the physicochemical behaviors have been studied by many mineralogists.[22–24] The high surface area, the charge on the lattice, and the inverted structure give attapulgites a high absorption capacity, which is of great benefit to be modified by long-chain organic cations. Although attapulgite has been widely used in drilling muds, paints, liquid detergents, adhesives, car polish, cosmetics, carriers for fertilizers and pet feed, etc., there are only a few reports about its use in nanocomposites up to now.[25,26]

In the present study, attapulgites were first modified by organic phosphonium and silane coupling agents, and then a series of PET/AT nanocomposites with different content of clay were prepared by *in situ* polycondensation. The dispersion, the crystallization, mechanical properties, and thermal properties of nanocomposites were studied in detail.

EXPERIMENTAL

Materials

Attapulgite clay (CEC = 25–30 mequiv/100 g, specific surface area 400–500 m^2/g) was obtained from Jiangsu Autobang International Co. (Xuyi County, Jiangsu, China). Hexadecyltriphenylphosphonium (HTPP)[27] bromide was synthesized and purified with regular procedures in our laboratory, and silane coupling agent (3-glycidoxypropltrimethoxysilane), acetic acid, zinc acetate, antimony trioxide, and ethylene glycol (EG) were purchased from Beijing Chemical Reagents Company (China). Dimethyl terephthalate (DMT) was a commercial product from Mitsubishi Chemical Corp. (Japan).

Preparation of organo-AT

A given weight of AT powder was dispersed uniformly in distilled water with vigorous stirring; the heavy mineral impurities such as quartz and dolomite were removed by precipitation. Then, the AT was separated by centrifugation. After dried *in vacuo* at 100°C for 4 h and ground into powder, attapulgites of 10 g (about 3 mmol of exchangeable cation) was introduced into 250 mL deionized water at room temperature. Then vigorous stirring and ultrasonic wave were applied to enhance the dispersion of clay. Hexadecyltriphenylphosphonium (5.0 g, 22.4 mmol) dissolved in 50 mL deionized water at 90°C was added into attapulgite suspension with vigorous stirring for 4 h. The resultant mixture was filtered and washed with distilled water three times to remove the residual salt. The obtained attapulgite slurry was added into the solution of acetic acid (PH = 3–4, 50 g) with the silane coupling agent of 0.2 g. After stirring vigorously for 30 min, the acquired attapulgite was dried in a vacuum for 4 h at 100°C and then milled to 300 mesh powders.

Synthesis of PET/attapulgite nanocomposites

100 parts of DMT by weight, 72 parts of EG by weight, a zinc acetate catalyst, and a given weight of organo-AT were introduced in a 500 mL four-neck flask with a nitrogen inlet and a mechanical stirrer. The reactor was heated under nitrogen atmosphere to 190°C, whereupon methanol was generated. After a theoretical amount of methanol was removed, an antimony trioxide catalyst was added to the reaction system and the temperature was raised to 260–280°C under a pressure of less than 30 Pa for 3 h. Then the polymerization was completed and PET/AT nanocomposite was obtained. Pure PET was synthesized under the same reaction conditions as mentioned already.

Measurements

X-ray diffraction

Wide angle X-ray diffraction (XRD) was performed on powders of organo-AT and slices of resins at room temperature by a Ragaku Model D/max-2B diffractometer at a generator voltage of 40 kV and a generator current of 100 mA. Testing data were collected from 1.5° to 40° at a scanning rate of 2°/min.

Fourier-transform infrared spectra

The clay particles were washed with acetone three times to remove the substances which were physically adsorbed on the surface of samples, and then dried at 100°C for 4 h. The dried clay powers were characterized by a Perkin–Elmer FTIR system 2000 spectrometer.

Scanning electron microscope

The morphology of the pure AT and organo-AT were inspected in scanning electron microscope (SEM) named HITACHI *S*-530. The clay powders were dispersed in water in ultrasonic bath for 20 min before the SEM examination.

Viscosity measurement

The intrinsic viscosity (η) of all samples was measured at 25°C in an Ubbelohde viscometers with the mixture of 50/50 (wt/wt) phenol/1,1,2,2-tetrachloroethane (TCE) as solvent.

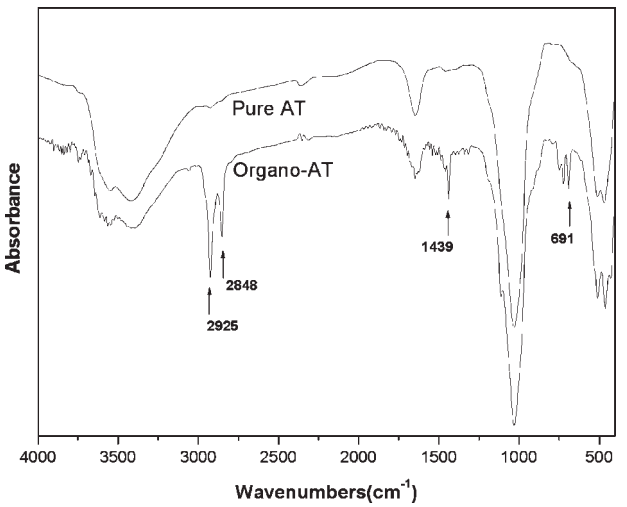

Figure 1 FTIR spectra of pure AT and the organo-AT.

Transmission electron microscope

The dispersion morphology of the fibrous clays in PET nanocomposites was investigated on a JEOL-100CX transmission electron microscope (TEM) using an acceleration voltage of 120 kV. All samples were microtomed by a diamond knife into 50–80 nm thick slices.

Thermogravimetric analysis

The thermal stability of organic-AT powders and PET/AT nanocomposites was characterized on a Perkin–Elmer 7 Series thermogravimetric analyzer, with samples being heated from 50 to 750°C in N_2 at a rate of 20°C/min.

Differential scanning calorimeter

The thermal properties of the PET/AT nanocomposites were examined with a Perkin–Elmer DSC-7 differential scanning calorimeter (DSC) thermal analyzer. Under nitrogen atmosphere, the samples of about 5.0 mg were heated from 50 to 300°C with a rate of 20°C/min and kept for 5 min at this temperature to remove the thermal history before cooling with a rate of 20°C/min.

Mechanical testing

The flexural tests of the composites were performed on a universal tensile tester (Instron 1122, UK) according to the standard method for testing the flexural properties of plastics (ASTM D790-97). The specimens for these tests were all prepared on an injection molding machine (SZ-15; Shanghai, China). The data reported here represent the average value of at least five successful tests.

RESULTS AND DISCUSSION

The characterization of organo-attapulgite

Because of the agglomeration of clay particles in the nanometer range, the pretreatment of attapulgite is important to improve sufficient dispersion of the clay in polymer matrix and adhesion of the PET main chains to this fibrous silicate, which resulted in the excellent performance of the PET/AT nanocomposites.[28] Attapulgite clay has a certain cation-exchange capacity, and many metal cations, such as the Na^+, Ca^{2+}, Mg^{2+}, Al^{3+}, rod-like crystals. These metal cations can be exchanged by long-chain organic cations. This organic modification is favorable to increase the affinity between the attapulgite clay and PET macromolecules. In addition, silane coupling agent with epoxy groups was used as clay surfactant, which can react with PET to improve adhesion between the inorganic phase and the matrix of polymer. The IR spectra of AT and Organo-AT are shown in Figure 1.

As shown in Figure 1 for the organo-AT and pure AT, there are major changes in the FTIR absorption peaks. Compared with the spectrum of pure AT, the new absorption peaks at 2925 and 2848 cm^{-1} are observed in the spectrum of organo-AT samples, which is due to the oscillation of C—H bond. The new absorptions at 1439 and 691 cm^{-1} are the character of phenyl group of triphenylphosphine salt, which confirms the organic modification of AT with Hexadecyltriphenylphosphonium bromide. In their spectra, the strong and wide absorption peaks of both organo-AT and pure AT in the higher wavenumber region at 3700–3200 cm^{-1} are ascribed to O—H stretching vibration. The sharp absorption peaks at 1035 cm^{-1} corresponds to the stretching vibration of Si—O bond.

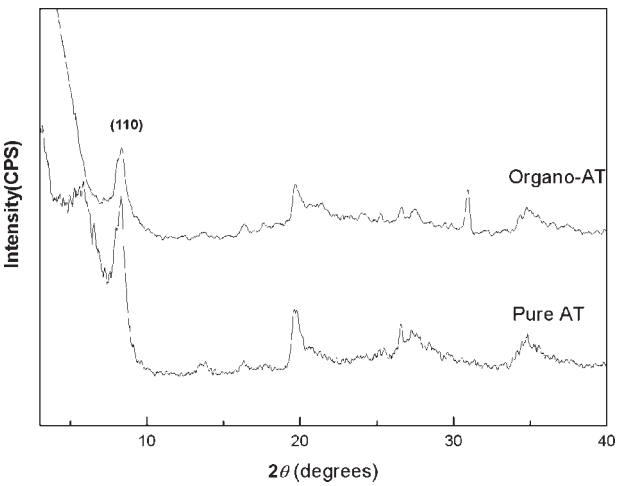

Figure 2 XRD patterns of pure AT and organo-AT.

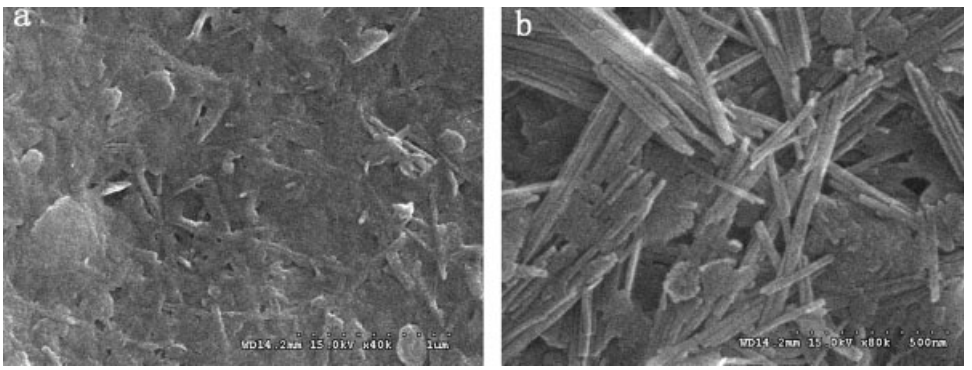

Figure 3 SEM images of (a) pure AT and (b) organo-AT.

In the powder XRD patterns of pure AT and organo-AT (Fig. 2), the location of the characteristic diffraction peak of attapulgite (110, $2\theta = 8.32$) did not shift. This indicates that organic modification was processed on the surface of rod-like crystals and did not change the crystal structure of attapulgite. This is different from layered clay such as montmorillonite, whose diffraction peak can shift to the lower 2θ range after organic modification. We attribute this to the difference of crystal morphology between attapulgite and montmorillonite. For montmorillonite, the periodic arrangement of the silicate layers both in pristine and in the intercalated states, within 1–4 nm, can be determined by X-ray diffraction conveniently. So in XRD patterns, the characteristic diffraction peak (001) of montmorillonite shifts to the lower 2θ range because the long-chain organic molecules, exchanged into the galleries of montmorillonite, can increase the basal distance between layers after organic modification. However, for AT, the characteristic diffraction peak (110) is due to the intrinsic axis structure of rod-like crystals. The organic modification only reduced the agglomeration of clay particles and cannot shift the structure of these rod-like crystals. Therefore, even the completely exfoliated rod-like crystals of AT hardly have an effect on the location of diffraction peak (110) in XRD pattern.

From SEM images in Figure 3, the morphology of attapulgite before and after organic modification can be observed directly. Just as shown in Figure 3 (a), because of the strong interaction between fibrous crystals in AT, pure AT agglomerated or bundled together with large scale, and it is difficult to find the single fibrous crystals. As shown in Figure 3(b), numerous single fibrous crystals can be observed clearly. This indicates that the interaction between the AT single crystal were weakened after organic modification, thus the large AT agglomerates could be broken down to primary particles. The diameter and length of single crystal is about 40 nm and 1000 nm, respectively. This high length-diameter ratio is favorable to enhance the polymer materials. In addition, from SEM images, it also can be found that organic modification was processed on the surface of AT and could not shift the fibrous crystal structure of AT, which corresponds to XRD patterns (Fig. 2).

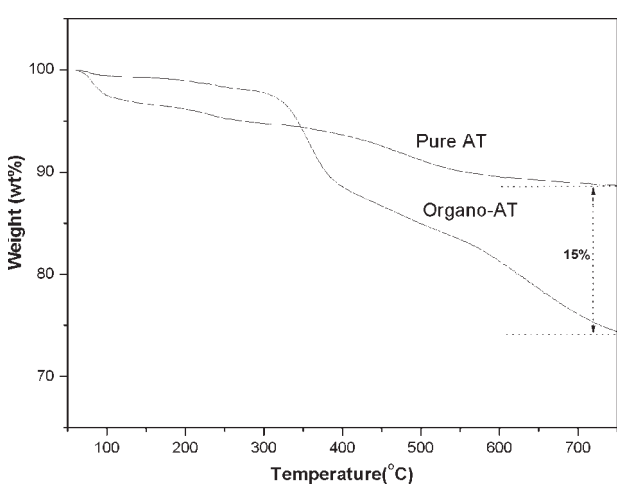

Figure 4 TGA curves of pure AT and organo-AT.

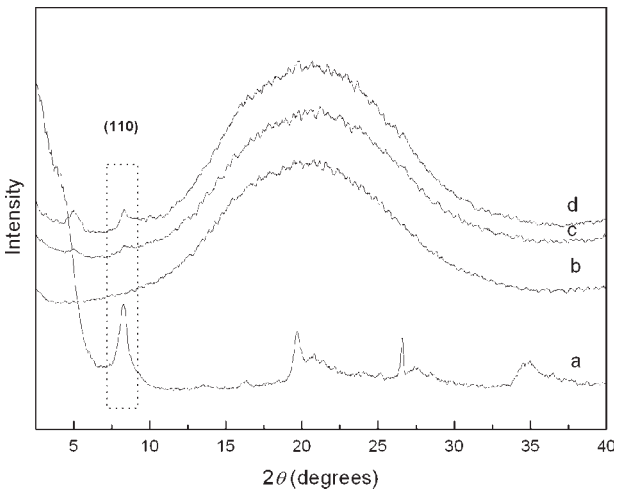

Figure 5 XRD patterns of (a) pure attapulgite, (b) pure PET, (c) PET/AT nanocomposite with 1 wt % AT loading, and (d) PET/AT nanocomposite with 3 wt % AT loading.

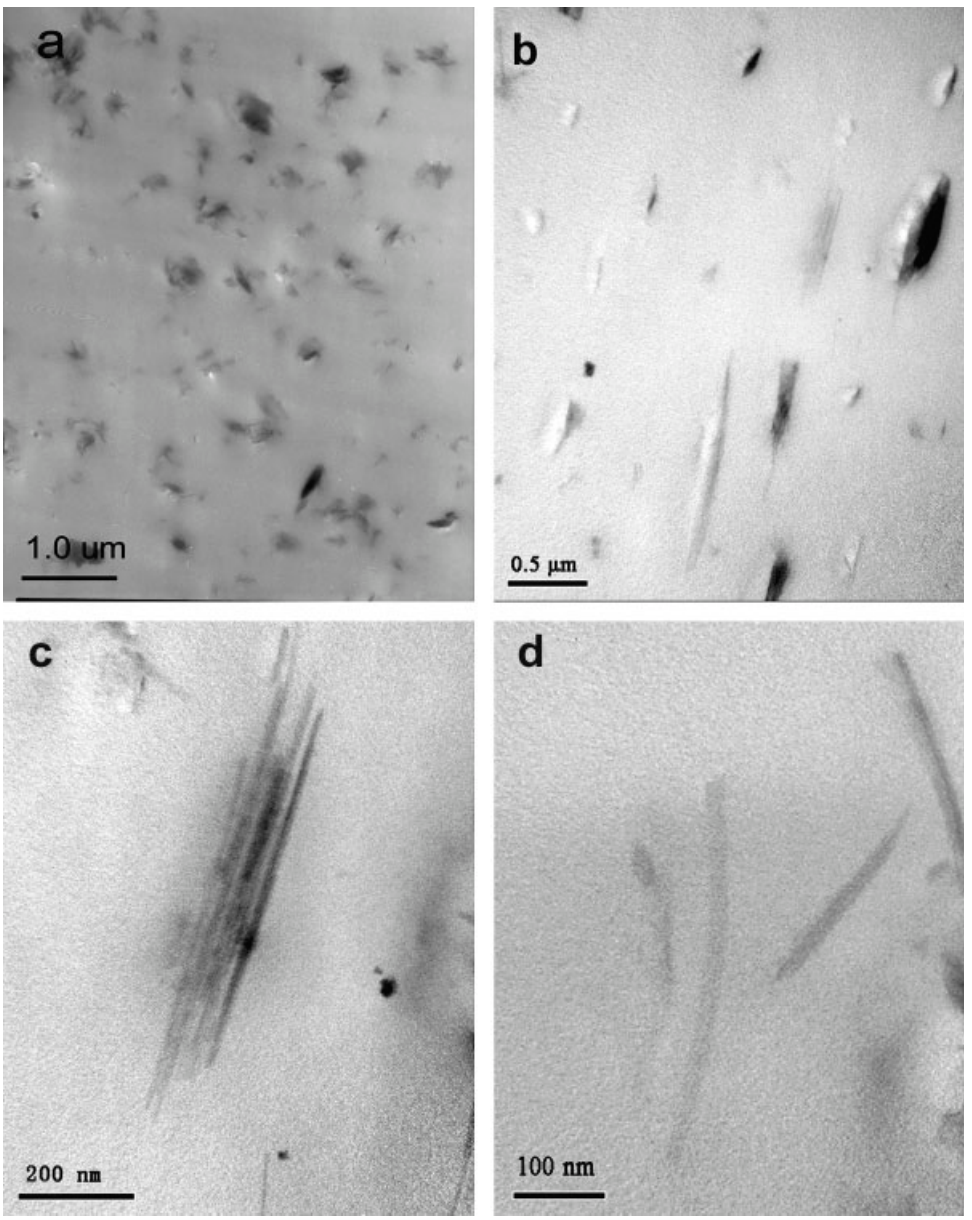

Figure 6 TEM of PET/AT nanocomposite with 1 wt % AT loading.

The synthesis and processing temperature of PET is so high (near 300°C) that some most widely used organic modifiers such as alkyl ammoniums have decomposed far below this temperature. The decomposition of modifiers may cause some negative effects on products,[11,12] and so the thermal stability of organic modifiers is very important for preparing PET/organo-AT nanocomposites. Thermogravimetric analysis in nitrogen atmosphere was used, in our research, to characterize the thermal stability of organo-AT, and the results are showed in Figure 4. The onset decomposition temperature (t_d) of organo-AT is around 320°C, which is an advantage for it to resist the high temperature during polycondensation and processing of PET. At 100°C, the weight loss of pure AT is about 4%, implying a loss of absorbed water.[29] At the temperature of 750°C, the weight loss of pure AT is 11%, but the weight loss of organo-AT has reached 26%. Thus we can calculate that the content of modifying agents in organo-AT is about 15%.

The properties of PET/AT nanocomposites

Figure 5 shows XRD patterns of attapulgite, PET, and two nanocomposites with different contents of AT. Pure attapulgite shows a strong peak at $2\theta = 8.32^\circ$, correspond to the primary diffraction of the (110) planes of the attapulgite. The pure PET has not peak at $2\theta = 8.32^\circ$, nevertheless PET/AT nanocomposites have the characteristic diffraction peaks (110) at $2\theta = 8.32^\circ$ of attapulgite. With the increase of clay content for nanocomposites, the intensity of the peak

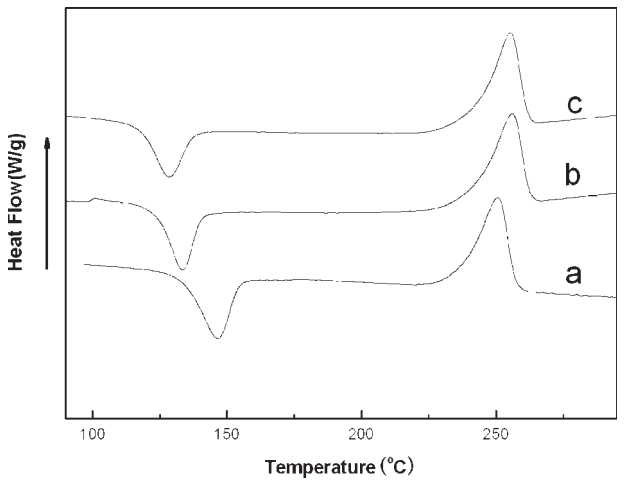

Figure 7 DSC heating thermograms of (a) pure PET, (b) PET/AT nanocomposite with 1 wt % AT loading, (c) PET/AT nanocomposite with 3 wt % AT loading.

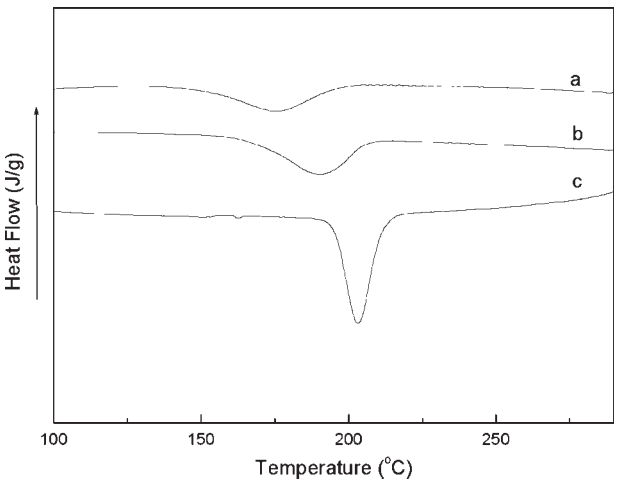

Figure 8 DSC cooling thermograms of (a) pure PET, (b) PET/AT nanocomposite with 1 wt % AT loading, (c) PET/AT nanocomposite with 3 wt % AT loading.

at $2\theta = 8.32^\circ$ enhances strongly. Even if the attapulgite in the PET/AT nanocomposites had been exfoliated to single rod-like crystals, the position of diffraction peak (110) of attapulgite at $2\theta = 8.32^\circ$ also did not change. Thus, it is hard to evaluate the dispersion of AT in polymer/AT nanocomposites through XRD test, which is different from that of polymer/layered clay nanocomposites.

The dispersion of AT in PET/AT nanocomposites could be observed from TEM. Usually, the two different magnifying powers are used to observe all-around dispersion morphology of nanocomposites. As shown in Figure 6(a), when the slices were measured at low magnifying power (10K), we can observe that the AT particles are well dispersed in the PET matrix, although some agglomerated particles still exist in the scale of several hundreds nanometers, and there are no agglomerated particles over the scale of micron. From Figure 6(b) (20K), we can observe that all the clay particles have the fibrous or rod-like form and the biggest thickness of agglomerated particles is below 300 nm.

Figure 6(c, d) were measured at high magnifying powers (100K), the rod-like crystals of AT could be observed clearly. As shown in Figure 6(c), several rod-like crystals of attapulgite are arrayed in parallel with the width of approximately 100 nm and the length about 500 nm. A little space between these rod-like crystals can be observed clearly and this morphology resembles the intercalated dispersion of layered clay nanocomposites. From Figure 6(d), it can be clearly observed that single rod-like crystals are dispersed in the PET matrix uniformly. The diameter of the individual rod-like crystal is about 20 nm and the length is near to 500 nm. According to the above results, the dispersion morphology of PET/organo-AT nanocomposites can be considered as a mixture of so-called intercalated and exfoliated structure. The uniform dispersion of AT in PET is of advantage to enhance the PET properties.

Lots of researchers have reported that the addition of silicate nanoparticles into polymer matrix increased the crystallization rate of polymers.[11,14,19] They explained that the clay particles dispersed uniformly in polymer matrix played a heterogeneous nucleating role that accelerated the crystallization rate of polymer. DSC heating and cooling scans at a rate of 20°C/min for PET and PET/AT nanocomposites with different AT contents are shown in Figures 7 and 8. The kinetic parameters of melting process and crystallization of these samples are listed in Table I. T_{cc}, T_m, and T_c represent cold crystallization temperature, apparent melting temperature, and crystallization temperature from melt, and the corresponding enthalpies are ΔH_{cc}, ΔH_m, and ΔH_c, respectively. Figure 7 shows that the neat PET exhibits a cold crystallization peak at about 146°C. In the case of nanocomposites with 1 and 3 wt % AT, the T_{cc} is lower than that of neat PET by 13°C and 18°C,

TABLE I
Properties of PET and PET/Organo-AT Nanocomposites

	AT content (wt %)		
	0	1.0	3.0
η (dl/g)	0.61	0.58	0.60
T_{cc} (°C)	146.4	133.3	128.3
ΔH_{cc} (J/g)	−32.9	−28.2	−25.4
T_m (°C)	250.8	255.6	255.1
ΔH_m (J/g)	36.9	43.1	38.6
T_C (°C)	175.1	190.4	203.2
ΔH_c (J/g)	−32.9	−38.1	−42.9
T_D (°C)	384	399	424
Flexural strength (MPa)	65	78	68
Flexural modulus (MPa)	1800	2230	2540

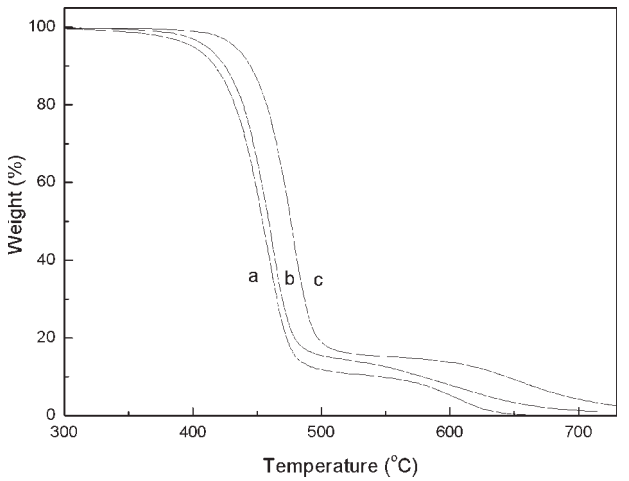

Figure 9 TGA curves of (a) pure PET, (b) PET/AT nanocomposite with 1 wt % AT loading, (c) PET/AT nanocomposite with 3 wt % AT loading.

respectively. This means that AT could act as heterogeneous nuclei of PET, which enhanced the crystallization rate of PET greatly.

During the cooling from the melt in Figure 8, all samples have one exothermic peak, but the crystallization temperature and shape of the crystalline peak had changed obviously. The presence of AT in the nanocomposites increased the crystallization temperature of PET and narrowed the width of the crystalline peak; meanwhile, the more the content of the AT, the higher the crystallization temperature was. This results also means that AT could act as heterogeneous nuclei of PET, which accelerated the rate of crystallization of PET greatly. This consists with other reports.

TGA analysis in nitrogen atmosphere was used to characterize the thermal stability of PET/organo-AT nanocomposites. Figure 9 shows the TGA thermograms of PET and PET/AT nanocomposites with different AT loading. The weigh loss onset temperature (T_{onset}) of pure PET, PET/AT nanocomposite with 1 wt % AT loading, and PET/AT nanocomposite with 3 wt % AT loading are about 384°C, 399°C, and 424°C, respectively. Compared with that of pure PET, PET/AT nanocomposites exhibited improved thermal stability, and the more the AT, the higher the weigh loss onset temperature of PET. The reason may be that strong interaction between polymer matrix and the particles of AT in nanometer range can restrict thermal motion of the PET molecules. Similar results of high thermal stability of PET/montmorillonite and PET/silica nanocomposites were reported by other scientists, although the fillers of nanocomposites are various and have different morphologies.[5,8,13,30]

The mechanical properties of the PET composites are also listed in Table I. It was found that the flexural modulus of the composites was enhanced significantly with the increase of AT content. The flexural modulus increased from 1800 MPa for pure PET to 2540 MPa for PET/AT nanocomposites with 3 wt % AT loading, which is an obvious increase of 41.1%. The enhancement of modulus for the PET/AT nanocomposites can be explained by Halpin–Tsai equations.[31] Acoording to the Halpin–Tsai equation, the modulus of hard particles is much higher than that of polymer matrices. Thus, the addition of the AT rod-liked crystals into polymers can afford higher modulus for composites.

CONCLUSIONS

In this article, a kind of clay with fibrous morphology, attapulgite, was used to synthesize PET nanocomposite via *in situ* polymerization. After attapulgites were modified with hexadecyltriphenylphosphonium bromide and silane coupling agent, the interaction between the AT single crystal was weakened. Differed with that of the layered clays, the dispersion morphology of attapulgite in polymer matrix cannot be shown by XRD test. However in fact, TEM revealed that attapulgite can be well dispersed with the rod-like crystals in PET matrix. The diameter of rod-like crystal is about 20 nm and the length is near to 500 nm. The thermal stability and crystallization rate of these nanocomposites were improved compared with those of pure PET. With the addition of AT in PET matrix, the flexural modulus of those composites was also increased markedly.

References

1. Okada, A.; Kawasumi, M.; Kurauchi, T.; Kamigaito, O. Polm Prepr 1987, 28, 447.
2. Kojima, Y.; Usuki, A.; Kawasumi, M.; Okada, A.; Fukushima, Y.; Kurauchi, T; Kamigaito, O. J Mater Res 1993, 8, 1185.
3. Yano, K.; Usuki, A.; Okada, A.; Kurauchi, T.; Kamigaito, O.; J Polym Sci Part A: Chem Mater 1993, 31, 2493.
4. Giannelis, E. P. Adv Mater 1996, 8, 29.
5. Ke, Y.; Long, C.; Qi, Z. J Appl Polym Sci 1999, 71, 1139.
6. Ke, Y.; Yang, Z.; Zhu, C. J Appl Polym Sci 2002, 85, 2677.
7. Wan, T.; Chen, L.; Chua, Y. C.; Lu, X. J Appl Polym Sci 2004, 94, 1381.
8. Ou, C.; Ho, M.; Lin, J. J Appl Polym Sci 2004, 91, 140.
9. Guan, G.; Li, C.; Zhang, D. J Appl Polym Sci 2005, 95, 1443.
10. Saujanya, C.; Imai, Y.; Tateyama, H. Polym Bull 2002, 49, 69.
11. Cabedo, L.; Giménez, E.; Lagaron, J. M.; Gavara, R.; Saura, J. J. Polymer 2004, 45, 5233.
12. Pan, Y.; Yu, Z.; Ou, Y.; Hu, G. J Appl Polym Sci 2000, 38, 1626.
13. Liu, W.; Tian, X.; Cui, P.; Li, Y.; Zheng, K.; Yang, Y. J Appl Polym Sci 2004, 91, 1229.
14. Qu, M.; Wang, Y.; Wang, C.; Ge, X.; Wang, D.; Zhou, Q. Eur Polym Mater 2005, 41, 2569.
15. Fray, M. E.; Boccaccini, A. R. Mater Lett 2005, 59, 2300.
16. Sreekumar, T. V.; Liu, T.; Min, B. G.; Guo, H.; Kumar, S.; Hauge, R. H.; Smalley, R. E. Adv Mater 2004, 16, 58.
17. Ma, H.; Zeng, J.; Realff, M. L.; Kumar, S.; Schiraldi, D. A. Compos Sci Technol 2003, 63, 1617.

18. Yusuke, I.; Satoshi, N.; Eiichi, A.; Hiroshi, T.; Akimasa, A.; Akira, Y.; Tomohiro, A.; Hiroaki, T. Chem Mater 2002, 14, 477.
19. Calvert, P. Nature 1999, 399, 210.
20. Song, Y. S.; Youn, J. R. Carbon 2005, 43, 1378.
21. Bradley, W. F. Am Mineral 1940, 25, 405.
22. Cao, E.; Bryant R.; Williams, D. J. A. J Colloid Interface Sci 1996, 179, 143.
23. Cao, E.; Yant, R. T.; Williams, D. J. A. Colloid Polym Sci 1998, 276, 842.
24. Haydn, M.; Min Miner Sustain Dev 2002, 64, 1.
25. Rong, J.; Sheng, M.; Li, H. Polym Compos 2002, 23, 658.
26. Kim, S. H.; Park, S.; Kim, S. C. Polym Bull 2005, 53, 285.
27. Zhu, J.; Morgan, A. B.; Lamelas, F. J.; Wilkie, C. A. Chem Mater 2001, 13, 3774.
28. Jang, B. N.; Wang, D.; Wilkie, C. A. Macromolecules 2005, 38, 6533.
29. Frost, R. L.; Ding, Z. Thermochim Acta 2003, 397, 119.
30. Chang, J.; Kim, S. J.; Joo, Y. L.; Im, S. Polymer 2004, 45, 919.
31. Halpin, J. C.; Kardos, J. L. Polym Eng Sci 1976, 16, 344.